The Plant Cell, Vol. 9, 2077–2091, November 1997 © 1997 American Society of Plant Physiologists

Early Events Induced by the Elicitor Cryptogein in Tobacco Cells: Involvement of a Plasma Membrane NADPH Oxidase and Activation of Glycolysis and the Pentose Phosphate Pathway

Alain Pugin,[a,1] Jean-Marie Frachisse,[b] Eric Tavernier,[a] Richard Bligny,[c] Elisabeth Gout,[c] Roland Douce,[c] and Jean Guern[b]

[a]Unité Associée, Institut National de la Recherche Agronomique/Université de Bourgogne, INRA BV 1540, 21034 Dijon Cedex, France

[b]Institut des Sciences Végétales, CNRS, 91198 Gif-sur-Yvette, France

[c]Physiologie Cellulaire Végétale et Résonance Magnétique en Biologie Métabolique, Département de Biologie Moléculaire et Structurale, Commissariat à l'Energie atomique (CEA), 17 rue des Martyrs, 38054 Grenoble Cedex 9, France

Application of the elicitor cryptogein to tobacco (cv Xanthi) is known to evoke external medium alkalinization, active oxygen species production, and phytoalexin synthesis. These are all dependent on an influx of calcium. We show here that cryptogein also induces calcium-dependent plasma membrane depolarization, chloride efflux, cytoplasm acidification, and NADPH oxidation without changes in NAD^+ and ATP levels, indicating that the elicitor-activated redox system, responsible for active oxygen species production, uses NADPH in vivo. NADPH oxidation activates the functioning of the pentose phosphate pathway, leading to a decrease in glucose 6-phosphate and to the accumulation of glyceraldehyde 3-phosphate, 3- and 2-phosphoglyceric acid, and phosphoenolpyruvate. By inhibiting the pentose phosphate pathway, we demonstrate that the activation of the plasma membrane NADPH oxidase is responsible for active oxygen species production, external alkalinization, and acidification of the cytoplasm. A model is proposed for the organization of the cryptogein responses measured to date.

INTRODUCTION

The interaction of *Phytophthora cryptogea* with tobacco cultivar Xanthi results in a hypersensitive reaction of the plant triggered by the proteinaceous elicitor cryptogein produced by the fungus (Billard et al., 1988; Ricci et al., 1989). Cryptogein elicits hypersensitive-like necroses on tobacco leaves and also protects the plant against various pathogens, especially *P. parasitica* var *nicotianae*.

For the past few years, we have been studying the mode of action of this elicitor by using tobacco cultivar Xanthi cell suspensions. We previously reported different effects of cryptogein on tobacco cells, including capsidiol and ethylene production (Milat et al., 1991), alkalinization of the extracellular medium and K^+ efflux (Blein et al., 1991), active oxygen species (AOS) production (Bottin et al., 1994), protein phosphorylation (Viard et al., 1994), changes in lipid composition (Tavernier et al., 1995a), calcium influx (Tavernier et al., 1995b), and early changes in gene expression (Suty et al., 1995; Petitot et al., 1997). Our results have led us to conclude that protein phosphorylation followed by calcium influx may be involved in the initial steps of cryptogein signal transduction (Tavernier et al., 1995b). Moreover, we have characterized specific high-affinity binding sites for cryptogein (K_d of 2 nM) in tobacco leaf plasma membranes (Wendehenne et al., 1995) and in plasma membranes from suspension-cultured tobacco cells (S. Bourque, A. Lebrun-Garcia, and A. Pugin, unpublished data).

The transient and fast production of AOS, including superoxide, H_2O_2, and the hydroxyl radical, by using cell suspensions treated with various elicitors is now well documented (Apostol et al., 1989; Sutherland, 1991; Bottin et al., 1994; Chen and Heath, 1994; Mehdy, 1994; Auh and Murphy, 1995; Tavernier et al., 1995b; Mathieu et al., 1996a). Whereas the antimicrobial activity of AOS has been recognized in animals, it is still not clear whether in plants, the AOS produced in response to pathogens or elicitors may have direct antimicrobial effects (Baker and Orlandi, 1995). They are assumed to be involved in other defense reactions, such as lipid peroxidation (Keppler and Novacky, 1987; Adam et al., 1989; Vera-Estrella et al., 1993; Stallaert et al., 1995), oxidative cross-linking of cell wall proteins (Bradley et al., 1992; Brisson et al., 1994), peroxidative polymerization of

[1]To whom correspondence should be addressed. E-mail pugin@epoisses.inra.fr; fax 33-03-80-63-32-65.

cinnamoyl alcohols leading to the lignification of cell walls (Hammerschmidt and Kuc, 1982; Kohle et al., 1984), and phytoalexin production (Doke, 1983; Apostol et al., 1989; Devlin and Gustine, 1992; Vera-Estrella et al., 1993). However, other results have shown that H_2O_2 is not a primary signal for phytoalexin production (Davis et al., 1993; Levine et al., 1994). Moreover, it has been reported that H_2O_2 from the oxidative burst triggers the hypersensitive death of challenged cells and functions in surrounding cells as a diffusible signal for induction of defense genes encoding enzymes involved in cellular protection (Levine et al., 1994; Tenhaken et al., 1995) or associated with systemic acquired resistance (Chen et al., 1993).

Many results indicate that $O_2^{\cdot -}$ synthesis occurs at the extracellular surface of the plasma membrane via a one-electron reduction of molecular oxygen (Doke, 1985; Auh and Murphy, 1995). For instance, Doke (1985) reported NADPH-dependent $O_2^{\cdot -}$ production by using microsomes from potato tubers infected by pathogen; in mammalian neutrophils, the production of superoxide $O_2^{\cdot -}$ as an antimicrobial agent involves a multicomponent NADPH oxidase that is assembled and functions at the plasma membrane (Babior, 1992; Segal and Abo, 1993). As previously reported (Rubinstein and Stern, 1986; Guern et al., 1988; Marré et al., 1988; Grabov and Böttger, 1994), the transfer of electrons from a cytosolic electron donor (NAD[P]H) to electron acceptors at the extracellular surface of the plasma membrane may lead to (1) an acidification of the cytosol due to the release of protons from the reducing agent; (2) an alkalinization of the extracellular medium due to the consumption of protons by different reactions (superoxide/hydroperoxide equilibrium [$O_2^{\cdot -} + H^+ \rightarrow HO_2\cdot$] and the dismutation of $O_2^{\cdot -}$ to H_2O_2 and O_2 either spontaneously or catalyzed with superoxide dismutases [$HO_2\cdot + O_2^{\cdot -} + H^+ \rightarrow H_2O_2 + O_2$; $2O_2^{\cdot -} + 2H^+ \rightarrow H_2O_2 + O_2$; Baker and Orlandi, 1995]); and (3) a decrease of the plasma membrane potential due to the electron transfer at the extracellular surface.

Thus, the activation of a plant plasma membrane redox system by pathogens or elicitors (Arnott and Murphy, 1991; Nürnberger et al., 1994; Tavernier et al., 1995b) may be responsible for cytosol acidification, previously reported in elicited cells (Ojalvo et al., 1987; Mathieu et al., 1991, 1996b), and plasma membrane depolarization, which is a common feature of elicited cells (Mathieu et al., 1991; Kuchitsu et al., 1993; Thain et al., 1995). These effects could participate in signal transduction and amplification.

Evidence supports the similarity of NAD(P)H oxidase in plant cells and NADPH oxidase in phagocytic animal cells involved in H_2O_2 production. In particular, antibodies raised against components of the neutrophil NADPH oxidase, responsible for the generation of $O_2^{\cdot -}$ during phagocytosis, cross-react with polypeptides of similar molecular masses in plants (Levine et al., 1994; Kieffer et al., 1997; Xing et al., 1997). Moreover, plant NAD(P)H oxidases are inhibited (Levine et al., 1994; Nürnberger et al., 1994; Dwyer et al., 1996) by diphenylene iodonium (DPI), a well-known inhibitor of the mammalian neutrophil oxidase (Cross and Jones, 1986). Nevertheless, no direct evidence indicates that NADPH is the substrate for this plant oxidase. In contrast, it was suggested that H_2O_2 could originate from other oxidases (Bolwell et al., 1995), because in many plant–elicitor interactions, the NADPH-to-NADP ratio remained constant during elicitation (Fahrendorf et al., 1995; Carpita et al., 1996).

By using phosphorus-31 nuclear magnetic resonance (^{31}P-NMR) to measure NADPH and $NADP^+$ levels and cytoplasmic pH changes, electrophysiological measurements to monitor plasma membrane potential, and selective electrodes to measure chloride efflux in cryptogein-treated tobacco cells, we show that cryptogein activates a plasma membrane NADPH oxidase whose activity depends on calcium influx and that is responsible for cytoplasm acidification but not for plasma membrane depolarization. NADPH oxidation activates the cytosolic pentose phosphate pathway, with the carbohydrate products being converted into glycolytic compounds that accumulate.

RESULTS

Cryptogein-Induced Cytoplasm Acidification and Calcium Dependence of the Response

^{31}P-NMR is a well-suited method for determining both changes in the pool size of endogenous phosphate compounds and intracellular pHs (Roberts and Jardetzky, 1981; Martin et al., 1982; Roby et al., 1987; Guern et al., 1989; Aubert et al., 1994).

Typical ^{31}P-NMR spectra of control and cryptogein-treated cells are illustrated in Figure 1. The peaks were assigned to specific compounds whose localization was deduced from the appropriate controls, taking into account the pH of the surrounding medium (Martin et al., 1982). In particular, two peaks of Pi were resolved at ~2.25 and 0.25 ppm corresponding to the cytoplasmic Pi and to the vacuolar Pi at pH 7.5 and pH 5.5, respectively. Other peaks were identified as cytoplasmic compounds: glucose 6-phosphate (Glc-6-P), fructose 6-phosphate (Fru-6-P), nucleoside triphosphates, and UDP-glucose (UDP-Glc). In addition, methylphosphonate, which accumulated inside cells from an external supply (see Methods), was also resolved in two peaks corresponding to vacuolar and cytoplasmic pools.

Ten minutes after the addition of 100 nM cryptogein in the circulating medium, the chemical resonance of the peak corresponding to the cytosolic Pi shifted from 2.25 to 2.0 ppm (Figure 1), indicating a 0.4 ± 0.1 (n = 3) pH unit acidification of the cytoplasm. No vacuolar pH change occurred during this period. The intensity of cytoplasmic acidification was confirmed and made more precise by using the change of the chemical shift of cytoplasmic methylphosphonate from 22.2 to 22.9 ppm, which corresponds to cytoplasmic pH of 7.5 and 7.05, respectively (pH drop of 0.45 ± 0.05; n = 3). On the other hand, cryptogein (100 to 500 nM) did not

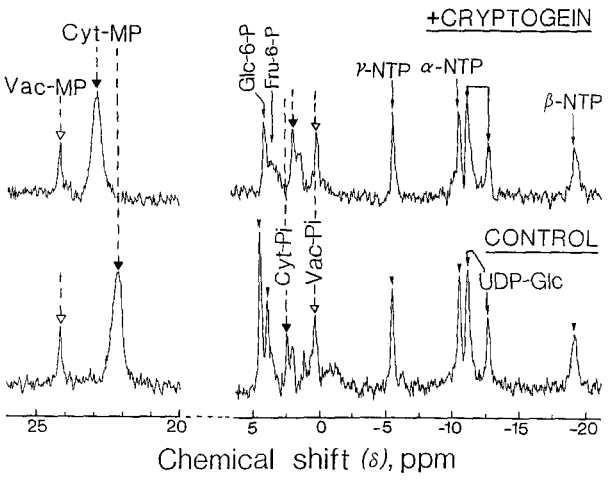

Figure 1. Representative Proton-Decoupled in Vivo ^{31}P-NMR Spectra (161.92 MHz) of Control and Cryptogein-Treated Tobacco Cells.

The cells (10 g wet weight) were packed in a 25-mm NMR tube, as described in Methods, and continuously perfused at a flow rate of 50 mL per min with a well-oxygenated manganese-free culture medium maintained at pH 6.5 and 20°C, as described by Roby et al. (1987). In the windows of analysis, the cell volume comprised ~50% of the total (cell plus perfusing medium) volume. The total perfusing medium was 500 mL. Spectra were recorded by using a multinuclear probe under the conditions given in Methods. Each spectrum is the result of 1000 scans cumulated over 10 min. The spectrum corresponding to cryptogein-treated cells was obtained 10 min after the addition of 100 nM cryptogein. Data are representative of three independent experiments. Peak assignments are as follows: Glc-6-P, glucose 6-P; Fru-6-P, fructose 6-P; Cyt-Pi, cytoplasmic phosphate; Vac-Pi, vacuolar phosphate; NTP, nucleoside triphosphate; UDP-Glc, uridine 5'-diphosphate-α-D-glucose; Cyt-MP, cytoplasmic methylphosphonate; and Vac-MP, vacuolar methylphosphonate.

induce any cytoplasmic acidification in *Acer pseudoplatanus* cells (data not shown), indicating that, as with the other effects of cryptogein, cytoplasmic acidification was specific to the tobacco cell–cryptogein interaction.

In the presence of 100 μM lanthanum, which is known to block the entrance of calcium into tobacco cells treated with cryptogein (Tavernier et al., 1995b), cryptogein did not induce any cytoplasmic acidification during a 2-hr treatment (data not shown), indicating that cytoplasmic acidification depends on the entrance of calcium.

Activation of an NADPH Oxidase

The spectra of cells treated with cryptogein for 10 min (Figure 1) also revealed a significant decrease in Glc-6-P concentration from 5 to 3 mM. This decrease in Glc-6-P could indicate activation of glycolysis and the tricarboxylic acid cycle (corresponding to an increased consumption of NADH) or of the pentose phosphate pathway (corresponding to an increased consumption of NADPH) or both.

^{31}P-NMR analysis of perchloric acid extracts prepared from 30-min–treated cells (at the end of the oxidative burst) and from control cells revealed that the NADPH-to-NADP$^+$ ratio, estimated from the upfield peaks of NADP$^+$ and NADPH located at 3.61 and 3.63 plus 3.64 ppm, respectively, strongly decreased in treated cells (Figure 2). Cytoplasmic NADPH levels decreased from 0.3 mM in control cells to 0.05 mM in treated cells, whereas the NAD$^+$ level (0.42 mM) did not change (see Table 1 and Methods for identifications and calculations). After perchloric acid extraction, NADH gave an upfield quadruplet, which overlapped with UDP-Glc and α-ATP peaks, like that of NADPH. Because NADH gives no upfield peak, it was not measurable.

Moreover, spectra analysis indicated a large accumulation in treated cells of products belonging to the second section of the glycolysis: glyceraldehyde 3-phosphate, 3-phosphoglyceric acid, 2-phosphoglyceric acid, and phosphoenolpyruvate, whereas the ATP levels did not change (Figure 2 and Table 1).

A similar decrease in NADPH level and a similar accumulation of glycolytic products were also measured in 15-min–treated cells during the oxidative burst. After a 1-hr treatment, cells partially recovered their initial status (data not shown).

These results clearly indicate that cryptogein induces a large oxidation of NADPH that leads to activation of the pentose phosphate pathway, whose first products are NADPH and ribulose 5-phosphate. NADPH is immediately oxidized by the plasma membrane oxidase, and ribulose 5-phosphate is converted into glyceraldehyde 3-phosphate and Fru-6-P. Both of these compounds are involved in glycolysis and/or glucose synthesis (Figure 3).

Origin of Cytoplasmic Acidification

To determine whether redox system activation was involved in cytosolic acidification and extracellular medium alkalinization, as suggested above, and to verify that NADPH was the electron donor, we inhibited the pentose phosphate pathway in two independent ways and monitored the consequences of these inhibitions on three effects of cryptogein, namely, H_2O_2 production, cytosolic acidification, and extracellular alkalinization.

The first enzyme of the pentose phosphate pathway is Glc-6-P dehydrogenase, which transforms Glc-6-P into 6-phosphogluconate. Glucosamine 6-phosphate (N-Glc-6-P) is a well-known competitive inhibitor of the enzyme (Glaser and Brown, 1955). To introduce the inhibitor into tobacco cells, 5 mM glucosamine was added for 1 hr to cell suspensions in place of glucose. Under this condition, cells took up glucosamine that was rapidly phosphorylated to N-Glc-6-P,

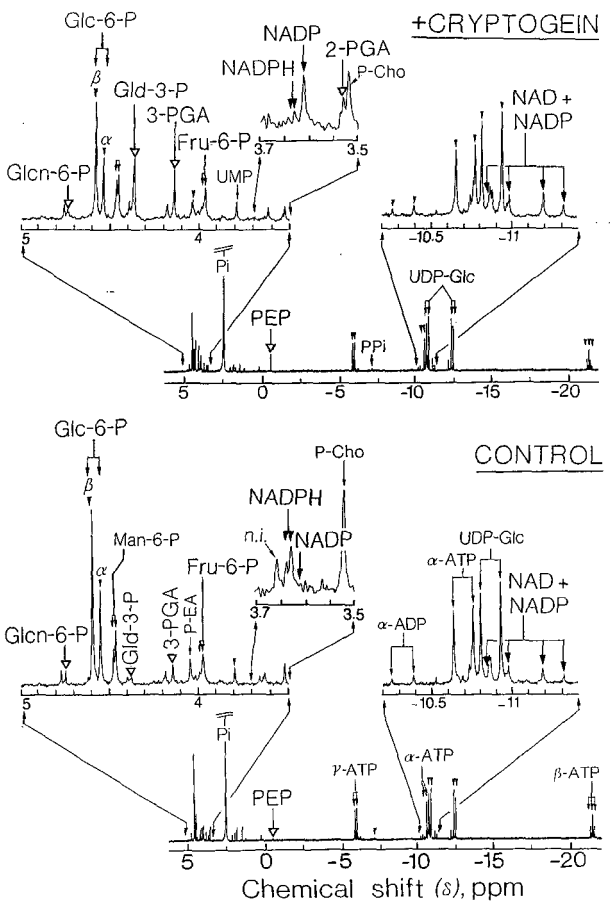

Figure 2. Representative Proton-Decoupled in Vitro ^{31}P-NMR Spectra (Perchloric Extracts, Expanded Scales from 5 to 3.5 ppm and from −10.2 to −11.4 ppm, between Arrows) of Control Tobacco Cells and Cells Incubated in the Presence of 50 nM Cryptogein for 30 Min.

Perchloric extracts were prepared from 9 g wet weight of cells, as described in Methods. The samples (3 mL) containing 300 μL of D_2O were analyzed for 8 hr (8192 scans) at 20°C with a 10-mm multinuclear probe tuned at 161.92 MHz. Data are representative of three independent experiments. Because of perchloric acid extraction, NADPH is transformed in a way giving upfield quadruplets, which are masked by UDP-Glc and α-ATP (see also Roberts et al., 1997). The downfield resonance of NADPH is split into two peaks at 3.63 and 3.64 ppm. $NADP^+$, which is not transformed by perchloric acid extraction, gives a downfield peak at 3.61 ppm and an upfield quadruplet at −10.87, −10.99, −11.19, and −11.31 ppm. The increase of the upfield quadruplet signal, which is identical to the increase of the downfield peaks, corresponds to $NADP^+$ production when, after addition of cryptogein, NADPH is oxidized in $NADP^+$. NAD^+, which is also stable after perchloric acid treatment and gives an upfield quadruplet superimposing exactly to that of $NADP^+$, remained constant. Peak assignments are as follows: Glc-6-P, glucose 6-P; Glcn-6-P, gluconate 6-P; Gld-3-P, glyceraldehyde 3-P; 3-PGA, 3-phosphoglyceric acid; 2-PGA, 2-phosphoglyceric acid; PEP, phosphoenolpyruvate; UDP-Glc, uridine 5′-diphosphate-α-D-glucose; UMP, uridine monophosphate; Fru-6-P, fructose 6-P; Man-6-P, mannose 6-P; P-EA, phosphorylethanolamine; P-Cho, phosphorylcholine; n.i, not identified. Open and solid arrowheads show intermediates of the glycolytic and pentose phosphate pathways and pyridine nucleotides, respectively.

as determined by ^{31}P-NMR spectra of perchloric acid extracts of treated cells (Figure 4). The large decrease in 6-phosphogluconate level (Figure 4) agrees with the expected inhibition of Glc-6-P dehydrogenase. Moreover, the NADPH-to-$NADP^+$ ratio estimated from perchloric acid extracts decreased strongly in glucosamine-treated cells (Table 2). In glucosamine-treated cells, cryptogein still induced calcium influx (Figure 5A) but did not induce any H_2O_2 production (Figure 5B), cytosolic acidification (data not shown), or extracellular alkalinization (Figure 5C).

These results favor an NADPH oxidase activated by the elicitor and responsible for AOS production, cytoplasmic acidification, and extracellular medium alkalinization. However, inhibiting the effects of cryptogein after treatment with glucosamine could be interpreted alternatively as an inhibition of elicitation by glucosamine itself, as previously reported with other monosaccharides (Basse et al., 1992, 1993), or by AOS scavenging. These alternative interpretations may be rejected because in the presence of 5 mM glucose, glucosamine was not taken up by the cells, and 100 nM cryptogein induced all of the previously described responses (data not shown).

In addition, to confirm the involvement of an NADPH oxidase in cryptogein-induced AOS production, cytoplasmic acidification, and extracellular medium alkalinization, experiments were performed using tobacco cells whose pentose phosphate pathways were inhibited in another way. It was previously reported that the addition of glycerol in place of sucrose in the culture medium of *A. pseudoplatanus* cells resulted in nonfunctioning of the cytosolic and plastidal pentose phosphate pathways (Aubert et al., 1994).

Thus, when tobacco cells were cultivated for 2 weeks in the presence of 50 mM glycerol in place of sucrose, the pentose phosphate pathway was not supplied with its initial substrate Glc-6-P. At that moment, the NMR analysis of perchloric acid extracts revealed that the NADPH-to-$NADP^+$ ratio was largely decreased (Table 2). Under these conditions, 100 nM cryptogein did not induce AOS production, cytosolic acidification, or extracellular medium alkalinization.

Moreover, when tobacco cells were treated with 25 μM DPI, an inhibitor of the mammalian neutrophil NADPH oxidase, 100 nM cryptogein did not induce AOS production and cytoplasmic acidification (data not shown). Taken together, these results indicate that the activation of the plasma membrane redox system responsible for H_2O_2 production was involved in cytosolic and extracellular pH modifications and that this redox system oxidized NADPH in vivo.

Table 1. Modifications of the Levels of Phosphorylated Compounds in Tobacco Cells Treated for 30 Min with 50 nM Cryptogein Measured Using ^{31}P-NMR Analysis[a]

Compounds	Glc-6-P	Fru-6-P	Man-6-P	Glcn-6-P	Gld-3-P	3-PGA	2-PGA	PEP	ATP	UDP-Glc	NAD^+	$NADP^+$	NADPH
Control	5.0	1.2	1.7	0.3	0.1	0.4	<0.05	0.2	2.2	3.4	0.42	<0.05	0.3
Cryptogein	3.0	1.3	1.2	0.15	2.2	1.0	0.15	0.9	2.0	3.4	0.42	0.3	<0.05

[a]Data are calculated from perchloric acid extracts, as indicated in Methods, and expressed as millimolar concentrations in the cytoplasm. Data are from a representative experiment (three assays). Abbreviations are as given in the legends to Figures 1, 2, and 4.

Plasma Membrane Depolarization, Chloride Efflux, and Calcium Dependence

The plasma membrane potential (E_m) of control tobacco cells was -153.8 ± 14.9 mV ($n = 5$). Figure 6A shows that the addition of 150 nM cryptogein depolarized the membrane to -35.6 ± 21.2 mV ($n = 5$). The whole depolarization occurred within 1 min, after a lag period of 4.3 ± 1.9 min. The addition of 250 μM lanthanum to the perfusion medium induced the repolarization of the membrane.

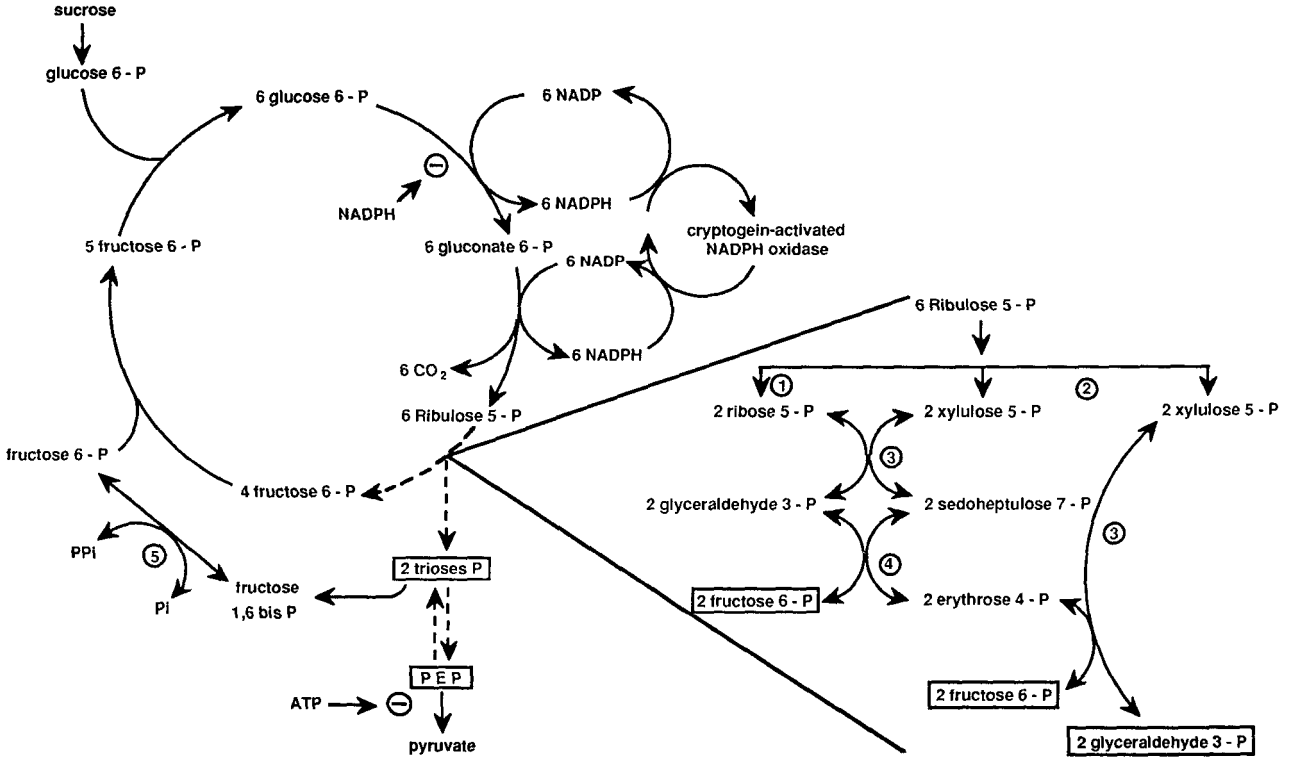

Figure 3. Schematic Representation of the Cytosolic Oxidative Pentose Phosphate Pathway Activated by Cryptogein to Supply the Demand for NADPH for $O_2^{\cdot-}$ Production at the Plasma Membrane.

The oxidative reactions of the pathway catalyzed by Glc-6-P dehydrogenase and phosphogluconate dehydrogenase both generate NADPH. These reactions are essentially irreversible. The reversible section of this pathway is involved in the regeneration of hexose phosphate and triose phosphates from ribulose 5-phosphate. The pentose phosphate pathway can bring about the complete breakdown of Glc-6-P to CO_2 if Fru-6-P and glyceraldehyde 3-phosphate (triose phosphate) are completely recycled. Recycling of triose phosphates requires the presence of a cytosolic pyrophosphate-linked phosphofructokinase. The most effective point of control of this pathway is at the initial step. Indeed, NADPH is a potent inhibitor of Glc-6-P dehydrogenase (competitive with respect to $NADP^+$). Finally, this scheme also explains the marked increase observed in the concentration of cytoplasmic glyceraldehyde 3-phosphate, 3-phosphoglyceric acid, and phosphoenolpyruvate during the rapid reoxidation of NADPH at the plasma membrane. Indeed, most of the reactions catalyzed by glyceraldehyde 3-phosphate dehydrogenase, phosphoglyceric acid kinase, phosphoglyceromutase, and enolase are close to equilibrium. Circled numbers indicate involved enzymes: 1, ribose-phosphate isomerase; 2, ribulose-phosphate epimerase; 3, transcetolase; 4, transaldolase; 5, PPi-linked phosphofructokinase. Dashed arrows indicate that intermediate compounds are not given.

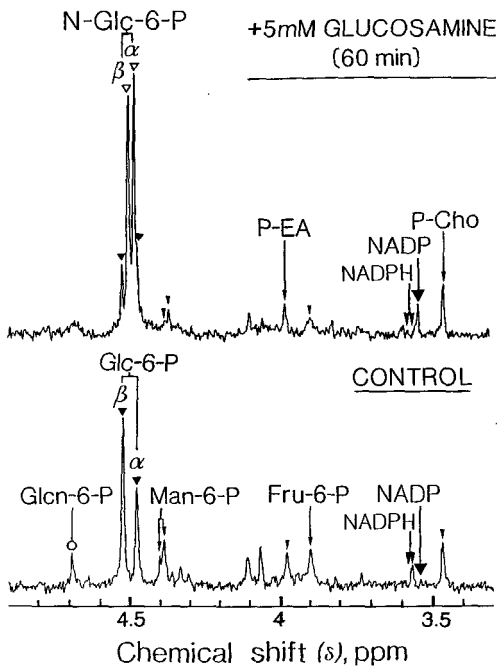

Figure 4. Representative Proton-Decoupled in Vitro ^{31}P-NMR Spectra (Perchloric Extracts, Expanded Scale from 4.8 to 3.4 ppm) of Control Tobacco Cells and Cells Incubated in the Presence of 5 mM Glucosamine for 60 Min.

Perchloric extracts were prepared from 9 g wet weight of cells, as described in Methods. The samples (3 mL) containing 300 μL of D_2O were analyzed for 1 hr (1024 scans) at 20°C with a 10-mm multinuclear probe tuned at 161.92 MHz, as detailed in Methods. Data are representative of three independent experiments. Peak assignments are as follows: *Glcn-6-P*, *gluconate* 6-P; *Glc-6-P*, *glucose* 6-P; *Fru-6-P*, *fructose* 6-P; Man-6-P, mannose 6-P; N-Glc-6-P, glucosamine 6-P; P-EA, phosphorylethanolamine; P-Cho; phosphorylcholine. $NADP^+$ (NADP) and NADPH peaks correspond to the 2′-P of this oxidized/reduced pyridine nucleotide. Open symbols indicate outstanding compounds in this assay.

In the same way, the addition of 250 μM lanthanum in the perfusion medium before cryptogein treatment prevented membrane depolarization (Figure 6B). Washing lanthanum from the medium while retaining cryptogein restored the cryptogein-induced depolarization. A second addition of lanthanum repolarized the membrane.

To verify whether the plasma membrane depolarization resulted from the activation of the plasma membrane redox system, we measured plasma membrane potential variation induced by cryptogein by using cells previously perfused for 30 min in the presence of 5 mM glucosamine. Under these conditions, in which the plasma membrane redox system was inhibited, 150 nM cryptogein induced the previously described depolarization (Figure 7A). Here, too, this depolarization was reversed by 250 μM lanthanum. Thus, the plasma membrane depolarization induced by cryptogein did not result from the plasma membrane redox system activation. This result was confirmed by treating tobacco cells with 25 μM DPI. Under these conditions, in which 150 nM cryptogein did not activate H_2O_2 production (data not shown), cryptogein induced a plasma membrane depolarization reversed by lanthanum (Figure 7B).

Because anion efflux could be involved in cryptogein-induced membrane depolarization, the influence of cryptogein on the exchanges of chloride was analyzed. Figure 8 shows that treating tobacco cells with 50 nM cryptogein induced a significant efflux of Cl^- (30 nmol of Cl^- per min per g fresh weight of cells). This efflux was strongly reduced (by ~90%) in the presence of 250 μM lanthanum, which blocks calcium entry.

None of these effects may be attributed to lethal effects of cryptogein. Indeed, using fluorescein diacetate and neutral red, we did not observe any dead cells during the first 3 hr of treatment with 100 nM cryptogein.

DISCUSSION

In this study, we provide evidence that the cryptogein-activated redox system, which is responsible for AOS production, oxidized NADPH in vivo. The activation of this plasma membrane NADPH oxidase is also responsible for the elicitor-induced cytoplasmic acidification and external medium alkalinization, at least during the initial phase of these responses. In contrast, cryptogein-induced membrane depolarization appears to be independent of the activation of this redox system. In addition, we observed that cryptogein did not induce a cytoplasmic pH change, extracellular medium alkalinization, or AOS production in *A. pseudoplatanus* cell suspensions, confirming the specificity of the tobacco–cryptogein interaction.

The large decrease in the NADPH-to-$NADP^+$ ratio in treated cells without significant changes in NAD^+ and ATP levels on the one hand and the large accumulation of glycolytic products on the other (Figure 2 and Table 1) clearly indicate that NADPH is the cofactor of the plasma membrane oxidase activated by cryptogein. The oxidation of NADPH by the plasma membrane redox system leads to the activation of the pentose phosphate pathway, which essentially is used for furnishing NADPH, with ribulose 5-phosphate being recycled in Fru-6-P and glyceraldehyde 3-phosphate. Fru-6-P is probably isomerized mainly in Glc-6-P that feeds the pentose phosphate pathway again, whereas glyceraldehyde 3-phosphate is converted in glycolytic products that accumulate (Figure 3). The large increase in glyceraldehyde 3-phosphate (from 0.1 to 2.2 mM), 2- and 3-phosphoglyceric acid, and phosphoenolpyruvate suggests that the activity of pyruvate kinase did not allow the further metabolization of the excess of phosphoenolpyruvate to respiration substrate. Indeed, the concentration of ATP, a potent inhibitor of pyruvate kinase, remained constant and high during cryptogein treatment.

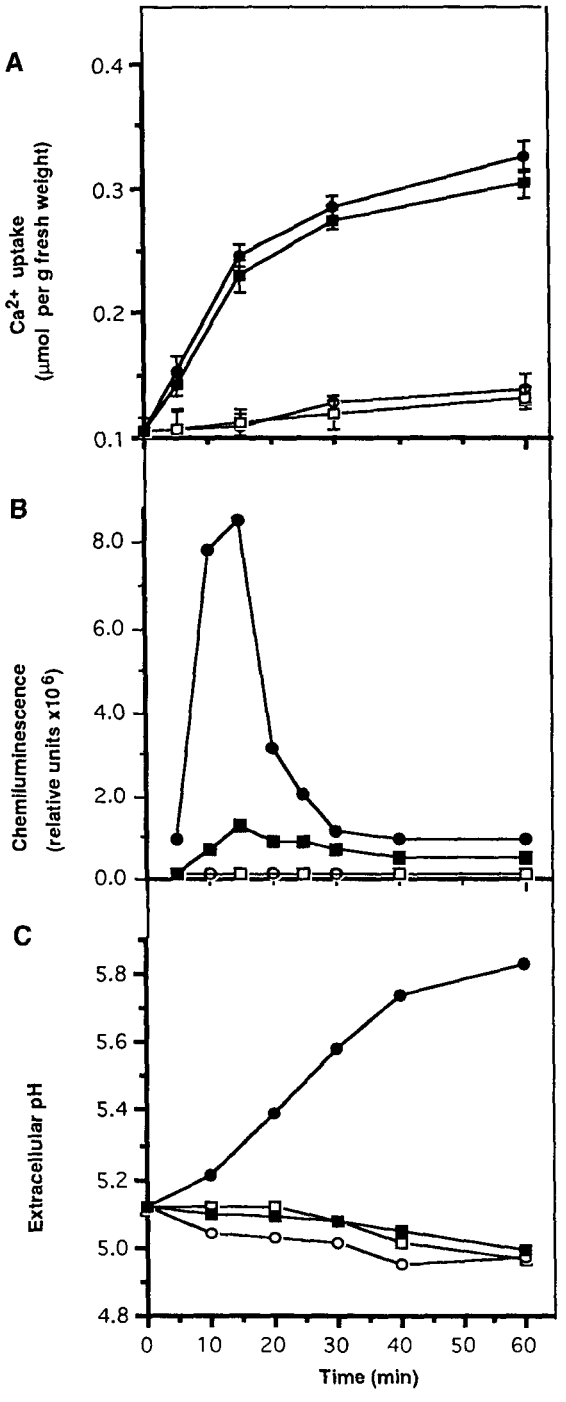

Figure 5. Calcium Influx, AOS Production, and Extracellular Alkalinization Induced by Cryptogein in Tobacco Cell Suspensions in the Presence or Absence of Glucosamine.

(A) Calcium influx.
(B) AOS production.
(C) Extracellular alkalinization.
(A) to **(C)** show induction by 50 nM cryptogein (dark symbols) in tobacco cell suspensions previously incubated for 1 hr in the presence (black squares) or absence (black circles) of 5 mM glucosamine. Control cells are with (open squares) or without (open circles) glucosamine. The data are representative of five experiments.

Table 2. Modifications of NADPH and $NADP^+$ Levels Induced in Tobacco Cells by Glucosamine Treatment of Glycerol Feeding and as Measured Using ^{31}P-NMR[a]

Treatment[a]	Control Cells	Glucosamine Treatment	Glycerol-Fed Cells
$NADP^+$	0.1 ± 0.05	0.30 ± 0.05	0.20 ± 0.08
NADPH	0.4 ± 0.1	ND[b] (<0.005)	ND[b] (<0.005)

[a]$NADP^+$ and NADPH were measured by ^{31}P-NMR from perchloric acid extracts, as indicated in Methods, and expressed as millimolar concentrations in the cytoplasmic compartment. The standard deviation is given for 90% from three different experiments.
[b]ND, not detected (<0.005 mM).

In contrast, the recycling of triose phosphates back to fructose 1,6-bisphosphate and further to Fru-6-P (from the back reaction of PPi-linked phosphofructokinase) was favored. Indeed, a rapid substrate cycle between the triose phosphates and the hexose phosphates was already observed in the cytosol of the heterotrophic *Chenopodium rubrum* cells by Hatzfeld and Stitt (1990). They also demonstrated that this cycle is due to the activity of the PPi-linked phosphofructokinase. Fructose 1,6-phosphatase activity is much too low to catalyze this back reaction. The magnitude of this back reaction would automatically respond to the needs of the oxidative pentose phosphate pathway. Thus, in contrast to Glc-6-P, Fru-6-P remained nearly constant (Table 1). Taken together, these results show that elicitation triggers a flux of carbohydrates from the pentose phosphate pathway to the lower and upper sections of the glycolysis with an active recycling toward Glc-6-P (Figure 3).

To provide further evidence concerning the oxidase cofactor in vivo and to evaluate the role played by the activation of the plasma membrane redox system in the induction of cytosolic acidification, we inhibited the pentose phosphate pathway in vivo or suppressed the supply of Glc-6-P to this pathway. The decrease in 6-phosphogluconate normally produced by Glc-6-P dehydrogenase and the decrease in the NADPH-to-$NADP^+$ ratio (Figure 4 and Table 2) confirmed the effective inhibition of the pentose phosphate pathway. Under these conditions in which calcium influx induced by cryptogein was not affected, three characteristic responses to the elicitor, namely, cytoplasmic acidification, external medium alkalinization, and AOS production, were

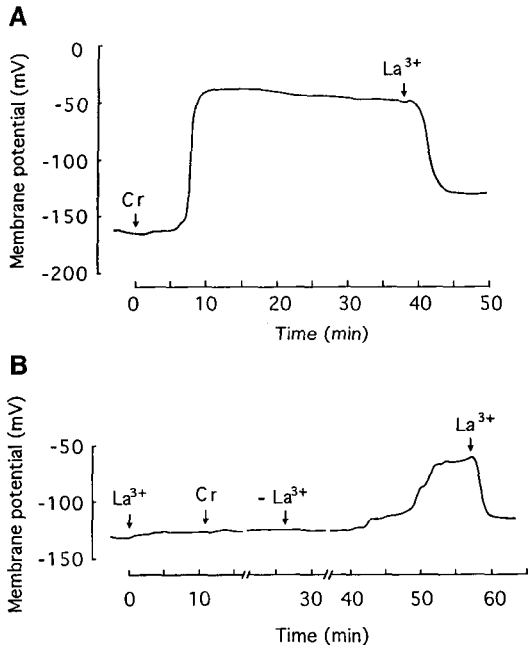

Figure 6. Tobacco Cell Plasma Membrane Depolarization Induced by Cryptogein and Its Inhibition by Lanthanum.

(A) The addition of 150 nM cryptogein (Cr; first arrow) depolarized the membrane to −40 mV after a lag period of 7 min. Treatment with 250 μM lanthanum (La^{3+}; second arrow) induced the repolarization of the membrane. Cells were equilibrated and continuously perfused during voltage measurements with a minimal medium (10 mM Mes, 5 mM sucrose, 0.5 mM $CaSO_4$, and 3 mM KOH, pH 5.7). Data are representative of four experiments.

(B) Lanthanum (250 μM) added to the perfusion medium (first arrow) prevented membrane depolarization by 150 nM cryptogein (second arrow). Washing lanthanum from the medium (third arrow) while keeping cryptogein in the perfusing medium restored the cryptogein-induced depolarization. A second addition of lanthanum (fourth arrow) repolarized the membrane. The same bath medium as given in **(A)** was used. Data are representative of four experiments.

abolished, indicating the involvement of the NADPH oxidase in pH modifications.

However, the time courses of pH changes and AOS production did not correlate, that is, alkalinization peaked long after the burst was over (Figure 5) and cytoplasmic acidification remained constant from 10 min to >1 hr. This suggests that additional mechanisms involved in pH regulation are mobilized in a second step to stabilize and/or amplify the pH changes due to the activity of the plasma membrane oxidase. For example, inhibition of the plasma membrane H^+-ATPase, by an excess of cytoplasmic calcium and/or after oxidation of thiol groups by AOS, could explain long-lasting pH changes. This assumption rests on the observation that ATP levels did not decrease in cryptogein-treated cells (Figure 1 and Table 1), whereas the large and sustained plasma membrane depolarization and cytoplasmic acidification should induce an activation of this ATPase (Gout et al., 1992), which is the major consumer of cellular ATP (Slayman et al., 1973; Sussman, 1994). The inhibition of AOS production by 5 μM DPI without the inhibition of the extracellular alkalinization in tobacco cell suspensions treated with cryptogein (Simon-Plas et al., 1997) is another example of the complexity of pH modifications induced by the elicitor. However, taken together, our results indicate that, besides H_2O_2 production, the activation of the tobacco plasma membrane redox system by cryptogein appears to be involved in cytoplasmic acidification and extracellular alkalinization.

NAD(P)H oxidoreductase activities associated with plasma membrane of both animal and plant cells have been demon-

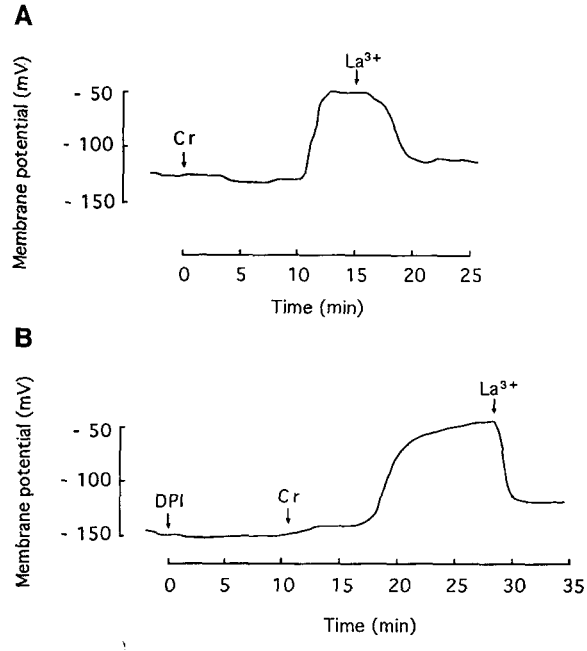

Figure 7. Effect of Glucosamine and DPI on the Membrane Depolarization Induced by Cryptogein.

(A) Glucosamine (5 mM) was added to the perfusion medium 30 min before cryptogein treatment. Cryptogein (Cr) (150 nM; first arrow) induced membrane depolarization that was reversed (second arrow) by lanthanum (La^{3+}). The bath medium is as given in the legend to Figure 6, except that glucose was replaced by mannitol. Data are representative of five experiments.

(B) The addition of 25 μM DPI to the perfusion medium (first arrow) was followed 10 min later by a 150-nM cryptogein treatment, which induced a membrane depolarization reversed by lanthanum (third arrow). The same bath medium as given in Figure 6 was used. Data are representative of five experiments.

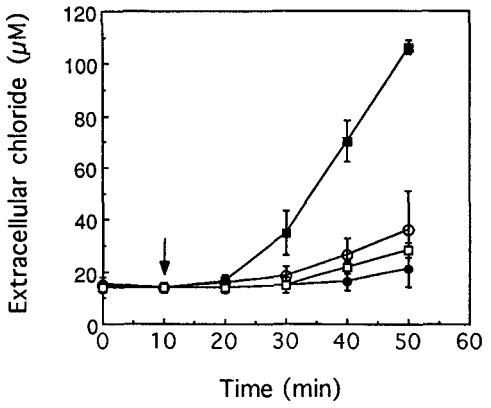

Figure 8. Time Course of Variations in External Chloride Concentration Induced by 50 nM Cryptogein in the Presence or Absence of 250 μM Lanthanum.

Cryptogein (50 nM) was added at time 10 min (arrow) in the absence (black squares) or presence (open squares) of 250 μM lanthanum added at time 0. Control cells were monitored in the absence (black circles) or presence (open circles) of lanthanum. Each curve is the mean ± SE of three independent experiments.

strated (Crane et al., 1988; Chanock et al., 1994). Despite increasing interest, very little is known about the proteins and the possible cofactors of these plant enzymes in vivo (Berczi and Asard, 1995).

An NADPH oxidase is present in lymphocytes and in the wall of the endocytic vacuole of phagocytic cells where oxidation of NADPH leads to the reduction of oxygen to superoxide and H_2O_2 (Rossi, 1986). The efficiency of this system resides in the alkalinization of vacuole lumen that results from electron transfer unaccompanied by protons and the consumption of protons in the vacuole lumen. This alkalinization activates neutral proteinases involved in pathogen digestion (Segal et al., 1981). The components of this redox system and the activation process are now well characterized (reviewed in Segal and Abo, 1993). Thus, in tobacco cells, the redox system activated by cryptogein resembles the NADPH oxidase of phagocytes more than it does the other plant plasma membrane oxidases, considering the electron donor, the electron acceptor, the transient activation, and the involvement in pH alterations. Moreover, tobacco cells contain a protein immunologically related to the neutrophil small G protein Rac2, which is involved in cryptogein-induced oxidative burst (Kieffer et al., 1997).

In animals it has been known for many years that changes in intracellular pH are involved in many processes such as cellular proliferation induced by growth factors (Isfort et al., 1993) or cell death (Greenspan and Aruoma, 1994). Specific inhibitors of vacuolar-type H^+-ATPase, which provoke cytosol acidification, also induce cell death (Nishihara et al., 1995).

In plant cells, cytosolic pH changes have been shown to be second messengers in signal transduction (Guern et al., 1991). The hypersensitive response to pathogens or elicitors, characterized by the appearance of necrotic lesions, is assumed to be a programmed cell death (Greenberg et al., 1994). Expression of a bacterial proton pump in transgenic tobacco plants activates a cell death program, with the appearance of lesions that resemble the hypersensitive response, and defense reactions (Mittler et al., 1995). Thus, cytoplasm acidification induced by cryptogein in tobacco plants could be a component of the signal cascade that leads to the hypersensitive response.

The activation of a plasma membrane redox system by extracellular ferricyanide has been shown to strongly depolarize cells of different plants (Marré et al., 1988). In neutrophils, activation of the plasma membrane oxidase triggers a membrane depolarization (Henderson et al., 1987). In tobacco cells, the depolarization still occurring when the redox system was inhibited by using DPI or glucosamine-treated cells (Figure 7) indicates that plasma membrane depolarization does not depend directly on the activation of the redox system.

The activation of calcium influx and chloride efflux (Figure 8) as well as an inhibition of the H^+-ATPase could contribute to the membrane depolarization. The large influx of calcium (10 ± 0.25 nmol of Ca^{2+} per g fresh weight of cells per min) corresponds to a depolarizing flux of charges quite similar to that carried by chloride ions (28.3 ± 1.8 nmol per g fresh weight of cells per min). The inhibition of chloride efflux by lanthanum suggests that the activation of the anion channel depends on the increase in cytoplasmic free calcium and/or on plasma membrane depolarization induced by calcium influx. Many results suggest now that anion channels along with calcium channels play a crucial role in early events of signal transduction (Schroeder and Hagiwara, 1989; Schroeder and Hedrich, 1989; Gilroy et al., 1990; Schroeder et al., 1993; Thuleau et al., 1994; Zimmermann et al., 1994, 1997; Schroeder, 1995; Ward et al., 1995; Gelli et al., 1997).

Figure 9 summarizes our results concerning the organization of the cryptogein responses, as revealed by preventing the massive calcium influx by staurosporine. After cryptogein perception and protein phosphorylation, the influx of calcium triggers two sets of responses: (1) anion efflux and H^+-ATPase inhibition resulting in plasma membrane depolarization and (2) the activation of a plasma membrane NADPH oxidase responsible for AOS production, cytoplasmic acidification, and extracellular medium alkalinization.

In conclusion, many responses of tobacco cells to the elicitor cryptogein have been characterized. Our work contributes to the understanding of the organization of this set of responses. A complex network of putative second messengers, including free calcium, cytosolic and extracellular pH changes, changes in membrane potential, generation of AOS, variations in redox state, and strong metabolic changes, is generated by the elicitor. The role(s) of possible second messengers, individually or in combination, should be more precisely investigated. Plasma membrane proteins, that is,

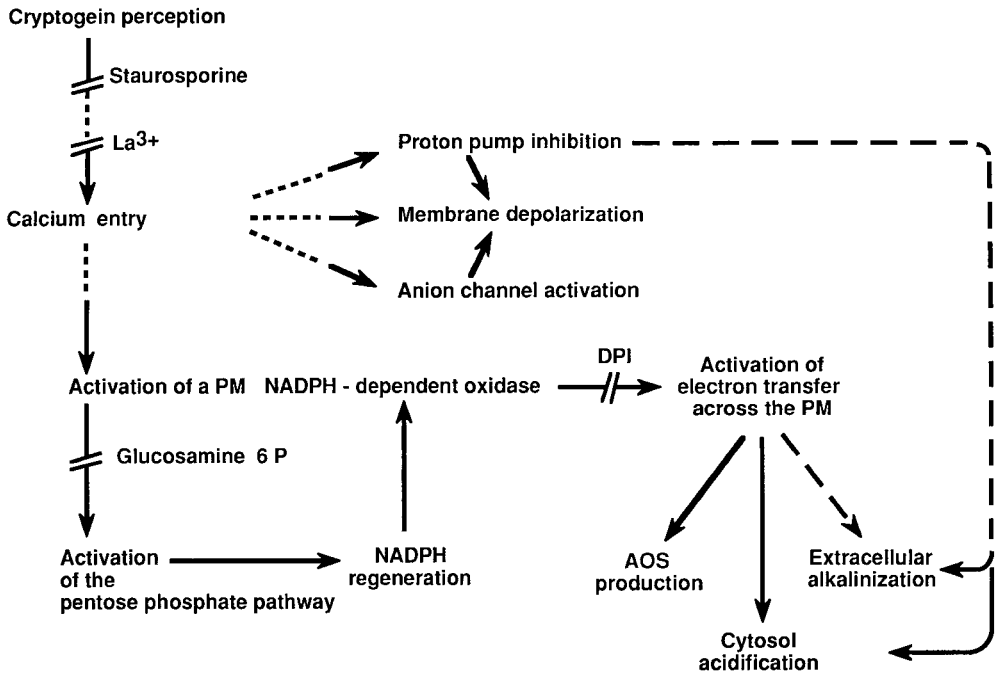

Figure 9. Proposed Model for the Organization of the Early Responses of Tobacco Cells to Cryptogein.

This tentative organization of the elicitor-induced events was built taking into account the effects of inhibitors (staurosporine for protein kinases, lanthanum and EGTA for calcium influx, and DPI, N-Glc-6-P (Glucosamine 6 P), and glycerol 3-phosphate for NADPH oxidase) and not the lag times of the responses, which depended heavily on the conditions of measurement of each response and on the sensitivity of the different methods used. Solid and broken arrows indicate established and hypothetical links, respectively, between events. La^{3+}, lanthanum; PM, plasma membrane.

calcium and anion channels, NADPH oxidase, and H^+-ATPase, which appear as key control proteins of the responses of tobacco cells, are now being investigated.

METHODS

Plant Material

Cell suspensions of *Nicotiana tabacum* cv Xanthi were grown in 250-mL conical flasks at 25°C and shaken at 150 rpm under constant light (Milat et al., 1991). The cells came from a culture of leaf tissue. Cell suspensions were subcultured every 7 days and used for elicitor treatment 5 days after subculturing. Cells were also cultivated in the presence of 100 mM glycerol as the sole source of carbon for 3 weeks. The culture medium was changed every 5 days. Cryptogein was purified according to Ricci et al. (1989) and added to cell suspensions as an aqueous solution.

Extracellular Alkalinization and Active Oxygen Species Production

Elicitor treatments were performed using 1 g fresh weight of cells in 10 mL of 2 mM Mes, 0.5 mM $CaCl_2$, 0.5 mM K_2SO_4, and 175 mM mannitol, pH 5.75, previously equilibrated for 2 hr. Extracellular pH was monitored for 1 hr after elicitor addition.

The production of active oxygen species (AOS) by cells was measured by chemiluminescence (luminometer Lumat 9501; Berthold, Bad Wilbad, Germany), using luminol as reagent. After the addition of cryptogein, aliquots of cell suspensions (250 μL) were added every 10 min to 350 μL of a 10-mM Mes buffer, pH 6.5, containing 175 mM mannitol, 0.5 mM $CaCl_2$, 0.5 mM K_2SO_4, and luminol (final concentration 25 μM). Chemiluminescence measurements were performed for 10 sec and expressed as H_2O_2 equivalents. Assays for monitoring H_2O_2 production were performed by adding different known amounts of H_2O_2 to cell suspensions, in the range of concentrations measured in experiments with cryptogein-treated cells. The increase in chemilumiscence was linearly proportional to the amount of H_2O_2 added between 15 and 150 μM.

Ca^{2+} Influx Measurements

Ca^{2+} uptake measurements were performed by the addition of $^{45}Ca^{2+}$ (0.033 MBq/g fresh weight of cells) 5 min before treatment with cryptogein. After various periods of treatment (0 to 90 min), duplicate samples of 3 mL were withdrawn by filtration and washed once for 1 min and twice for 20 sec on GF/A glass microfiber filters (Whatman) with 10 mL of ice-cold 2 mM $LaCl_3$ in assay medium without Ca^{2+} to remove extracellular $^{45}Ca^{2+}$. Cells were scraped from the filters, placed in scintillation vials, and weighed. Ten milliliters of

Ready Safe cocktail (Beckman Instruments, Fullerton, CA) was added to the vials, which were gently shaken overnight before counting in a scintillation counter (model LS 600 TA; Beckman Instruments).

In a second step, Ca^{2+} net uptake was measured by flame photometry (AA 300; Varian, Melbourne, Australia). The experiments were performed as described above without $^{45}Ca^{2+}$. The decrease in extracellular Ca^{2+} was measured in the assay medium after filtration.

Chloride Efflux Measurements

To study the efflux of Cl^-, a 5-day-old tobacco cell suspension was equilibrated for 5 hr in 10 mM Mes, 5 mM sucrose, 0.5 mM $CaSO_4$, and 3 mM KOH, pH 5.7, at ~100 mg fresh weight of cells per mL. After treatment with cryptogein and other effectors, 3.5 mL of the cell suspension was sampled every 10 min and filtered. A 2-mL aliquot of filtrate was adjusted to 0.1 M sulfate with 0.5 M K_2SO_4, and its chloride activity was monitored using a Cl^- specific electrode (XS 21 Tacussel; Radiometer, Copenhagen, Denmark) connected with a mercurious sulfate ($Hg/Hg_2SO_4/K_2SO_4$) reference electrode to a ION 85 ionometer (Radiometer). The potential of the Cl^- specific electrode relative to the reference was linear (58 mV decade^{-1}) for Cl^- concentrations $>10^{-4}$ M. For each experiment, the electrode was calibrated within a range of 10^{-6} to 10^{-3} M Cl^- with KCl. The Cl^- concentration of the medium was determined by using the calibration curve.

In Vitro Phosphorus-31 Nuclear Magnetic Resonance Measurements

Perchloric Extract Preparation

Cells (9 g fresh weight) were quickly frozen in liquid nitrogen and ground to a fine powder with a mortar and pestle with 1 mL of 70% (v/v) perchloric acid. The frozen powder was then placed at −10°C and thawed. The thick suspension thus obtained was centrifuged at 15,000*g* for 10 min. The supernatant was neutralized with 2 M $KHCO_3$ to approximately pH 5 and then centrifuged at 10,000*g* for 10 min to remove $KClO_4$. The resulting supernatant was lyophilized and stored in liquid nitrogen. This freeze-dried material was redissolved in 2.5 mL of water containing 10% heavy water (D_2O) neutralized to pH 7.5 and buffered with 50 mM Hepes. Divalent cations (particularly Mn^{2+} and Mg^{2+}) were chelated by the addition of 1,2-cyclohexylenedinitrilotetraacetic acid ranging from 50 to 100 mmol.

Nuclear Magnetic Resonance Measurements

Phosphorus-31 nuclear magnetic resonance (^{31}P-NMR) spectra of neutralized perchloric acid extracts were obtained on an NMR spectrometer (model AM 400, narrow bore; Bruker, Wissenbourg, France) equipped with a 10-mm multinuclear probe tuned at 161.92 MHz. Acquisition used 70° pulses at 3.6-sec intervals. The deuterium resonance of D_2O was used as a lock signal, and the spectra were recorded over a period of 1 hr (1024 scans), or 8 hr when necessary, under conditions of broad-band proton decoupling (Waltz pulse sequence at a sweep width of 6000 Hz). An exponential multiplication (0.2-Hz line width) was used to increase signal-to-noise ratio. Perchloric acid extract spectra are referenced to methylene diphosphonic acid, pH 8.9, at 16.38 ppm. The spectra of standard solutions of known phosphate compounds at pH 7.5 were compared with that of a perchloric acid extract of *Acer pseudoplatanus* cells. The definitive assignments were made after running a series of spectra obtained by addition of the authentic compounds to the perchloric acid extracts, according to previous publications (Roby et al., 1987; Aubert et al., 1994).

For the identification and quantification of pyridine nucleotides, perchloric acid–pretreated compounds were used. To determine accurately the total amount of the most abundant soluble organic compounds present in the perchloric extracts, we proceeded as follows: (1) 20-sec recycling time was used to obtain fully relaxed spectra; and (2) a calibration of the peak intensities was measured by integration of peak areas after the addition of known amounts of the corresponding authentic compounds. In addition, we took into account the extraction rate of the perchloric extraction. By adding known amounts of authentic compounds to the frozen cells before grinding, we estimated that the overall yield of recovery was 75 to 80%.

$NADP^+$ and NADPH were measured by ^{31}P-NMR from the downfield $NADP^+$ and NADPH singlets at 3.61 and 3.63 plus 3.64 ppm, respectively. It should be stressed that NADPH is transformed by perchloric acid extraction in a way that splits and slightly shifts the downfield peak and gives upfield quadruplets between −10.6 and −11 ppm, overlapping with UDP-glucose (UDP-Glc) and α-ATP peaks, which consequently cannot be used for quantification as shown for mitochondrial extracts (Roberts et al., 1997). In contrast, oxidized pyridine nucleotides ($NADP^+$ and NAD^+) are not modified by perchloric acid extraction, giving an upfield quadruplet at −10.87, −10.99, −11.19, and −11.31 ppm. NAD^+ was measured from the upfield NAD^+ plus $NADP^+$ quartet after subtraction of the contribution of $NADP^+$ calculated from the downfield peak of $NADP^+$ (at 3.61 ppm). Concentrations were estimated assuming that these compounds are present exclusively in the cytoplasm and that the cytoplasm occupies nearly 10% of the total cell volume, as described by Aubert et al. (1994).

In Vivo ^{31}P-NMR Measurements

Ten grams fresh weight of tobacco cells was slightly compressed in a 25-mm NMR tube and perfused under slight pressure at a flow rate of 50 mL per min with a well-oxygenated (O_2 bubbling) nutrient medium (0.5 mM KCl, 0.5 mM KNO_3, 0.5 mM $MgSO_4$, 1 mM $Ca(NO_3)_2$, 0.1 mM KH_2PO_4, and 2 mM sucrose, pH 6.3). After 2 hr of equilibration, 100 nM cryptogein was added in this circulating medium. The pH of this medium (500 mL) was maintained constant by using a pH stat coupled to a titrimeter monitoring the addition of registered amounts of HCl or KOH.

To get a better signal-to-noise ratio, an experimental arrangement was realized to analyze the maximum cell volume and to optimize the homogeneity of the cell incubation conditions (Roby et al., 1987). ^{31}P-NMR spectra were measured on a spectrometer (AMX 400, wide bore; Bruker) equipped with a 25-mm probe tuned at 161.92 MHz. Acquisition used 50° pulses at 0.6-sec intervals, and free induction decays were recorded with 8000 data points and zero filled to 16,000 before Fourier transformation. A 20-sec recycling time was used to obtain fully relaxed spectra necessary for quantitative measurements. The deuterium resonance of D_2O was used as a lock signal, and the spectra were recorded over a period of 10 min (1000 scans) under conditions of broad-band proton decoupling (Waltz pulse sequence) at a sweep width of 6000 Hz. An exponential multiplication (5-Hz line width) was used to increase the signal-to-noise ratio. Spectra are referenced to a solution of 50 mM methylene diphosphonic

acid (pH 8.9 in 30 mM Tris) contained in a 0.8-mm capillary inserted inside the inlet tube along the symmetry axis of the cell sample (Roby et al., 1987).

The intracellular pH values were first estimated from the intracellular Pi pools (cytoplasm and vacuole), as indicated by Gout et al. (1992). In addition, methylphosphonate added at a concentration of 1 mM for 6 hr in the culture medium was also used as a convenient probe for the precise determination of cytoplasmic pH. Indeed, methylphosphonate has a chemical shift sensitivity to pH nearly twice that of Pi, a pKa of 7.6, and it resonates between 20 and 25 ppm in a region usually devoid of other phosphorus-31 resonances. For this reason, it has already been used successfully with other materials (Slonczewski et al., 1981; Satre et al., 1989).

The assignment of Pi, phosphate esters, phosphate diesters, and nucleotides to specific peaks was performed according to the methods of Roberts and Jardetzky (1981), Roby et al. (1987), and Aubert et al. (1994) and from spectra of the perchloric acid extracts that contained the soluble low molecular weight constituents. Finally, when given, intracellular concentrations were calculated on the following basis: 1 g cell wet weight corresponds to 1 mL cell volume and ~0.10 mL cytoplasm.

Measurement of Membrane Potentials

A 5-day-old tobacco cell suspension was equilibrated during 3 hr in 10 mM Mes, 5 mM glucose, 0.5 mM $CaSO_4$, and 3 mM KOH, pH 5.7. To immobilize cells, the cut section of a 3-mm-long capillary was covered with a thin layer of lanolin and then dipped into the cell suspension. The capillary with immobilized cells at its section was fixed at the bottom of a perfusion chamber.

Micropipettes were pulled with a vertical puller (model PA-81; Narishige, Tokyo, Japan) from filament containing borosilicate glass (model GC 150F-15; Clark, Pangbourne, UK). The reference electrode (positioned downstream in the perfusion chamber) and the micropipette were filled with 0.5 M KCl. The resistance of the microelectrode was $\sim 30.10^6$ ohms. The electrodes were connected via Ag/AgCl wires to a high-impedance electrometer amplifier (model 8700 cell explorer; Dagan, Minneapolis, MN). The voltage changes were recorded with a pen chart recorder.

The chamber (2-mL volume) was continuously perfused at a rate of 2.5 mL per min. After impalement, when a stable membrane potential was obtained for several minutes, the bath solution was supplemented with the different effectors to be tested.

ACKNOWLEDGMENTS

We thank Dr. Pierre Ricci for the generous gift of cryptogein and Annick Chiltz for excellent technical assistance.

Received June 10, 1997; accepted September 26, 1997.

REFERENCES

Adam, A., Farkas, T., Somlyai, G., Hevesi, M., and Kiraly, Z. (1989). Consequence of $O_2^{\cdot-}$ generation during a bacterially induced hypersensitive reaction in tobacco: Deterioration of membrane lipids. Physiol. Mol. Plant Pathol. **34,** 13–26.

Apostol, I., Heinstein, P.F., and Low, P.S. (1989). Rapid stimulation of oxidative burst during elicitation of cultured plant cells. Role in defense and signal transduction. Plant Physiol. **90,** 109–116.

Arnott, T., and Murphy, T.M. (1991). A comparison of the effects of a fungal elicitor and ultraviolet radiation on ion transport and hydrogen peroxide synthesis by rose cells. Environ. Exp. Bot. **31,** 209–216.

Aubert, S., Gout, E., Bligny, R., and Douce, R. (1994). Multiple effects of glycerol on plant cell metabolism. J. Biol. Chem. **269,** 21420–21427.

Auh, C.K., and Murphy, T.M. (1995). Plasma membrane redox enzyme is involved in the synthesis of $O_2^{\cdot-}$ and H_2O_2 by *Phytophthora* elicitor-stimulated rose cells. Plant Physiol. **107,** 1241–1247.

Babior, B.M. (1992). The respiratory burst oxidase. Adv. Enzymol. Relat. Areas Mol. Biol. **65,** 49–88.

Baker, C.J., and Orlandi, E.W. (1995). Active oxygen in plant pathogenesis. Annu. Rev. Phytopathol. **33,** 299–321.

Basse, W.C., Bock, K., and Boller, T. (1992). Elicitors and suppressors of the defense response in tomato cells. Purification and characterization of glycopeptide elicitors and glycan suppressors generated by enzymatic cleavage of yeast invertase. J. Biol. Chem. **267,** 10258–10265.

Basse, W.C., Fath, A., and Boller, T. (1993). High affinity binding of a glycopeptide elicitor to tomato cells and microsomal membranes and displacement by specific glycan suppressors. J. Biol. Chem. **268,** 14724–14731.

Berczi, A., and Asard, H. (1995). NAD(P)H-utilizing oxidoreductases of the plasma membrane—An overview of presently purified proteins. Protoplasma **184,** 140–144.

Billard, V., Bruneteau, M., Bonnet, P., Ricci, P., Pernollet, J.C., Huet, J.C., Vergne, J.C., Richard, G., and Michel, G. (1988). Chromatographic purification and characterization of elicitors of necrosis on tobacco produced by incompatible *Phytophthora* species. J. Chromatogr. **44,** 87–94.

Blein, J.P., Milat, M.L., and Ricci, P. (1991). Responses of cultured tobacco cells to cryptogein, a proteinaceous elicitor from *Phytophthora cryptogea*: Possible plasmalemma involvement. Plant Physiol. **95,** 486–491.

Bolwell, G.P., Butt, V.S., Davies, D.R., and Zimmerlin, A. (1995). The origin of the oxidative burst in plants. Free Radical Res. **23,** 517–532.

Bottin, A., Véronési, C., Pontier, D., Esquerré-Tugayé, M.T., Blein, J.P., Rusterucci, C., and Ricci, P. (1994). Differential responses of tobacco cells to elicitors from two *Phytophthora* species. Plant Physiol. Biochem. **32,** 373–378.

Bradley, D.J., Kjellbom, P., and Lamb, C.J. (1992). Elicitor-induced and wound-induced oxidative cross-linking of a proline-rich plant cell wall protein—A novel, rapid defense response. Cell **70,** 21–30.

Brisson, L.F., Tenhaken, R., and Lamb, C. (1994). Function of oxidative cross-linking of cell wall structural proteins in plant disease resistance. Plant Cell **6,** 1703–1712.

Carpita, N., McCann, M., and Griffing, L.R. (1996). The plant extracellular matrix: News from the cell's frontier. Plant Cell **8,** 1451–1463.

Chanock, S.J., Elbenna, J., Smith, R.M., and Babior, B.M. (1994). The respiratory burst oxidase. J. Biol. Chem. **269,** 24519–24522.

Chen, C.Y., and Heath, M.C. (1994). Features of the rapid cell death induced in cowpea by the monokaryon of the cowpea rust fungus or the monokaryon-derived cultivar-specific elicitor of necrosis. Physiol. Mol. Plant Pathol. **44,** 157–170.

Chen, Z.X., Silva, H., and Klessig, D.F. (1993). Active oxygen species in the induction of plant systemic acquired resistance by salicylic acid. Science **262,** 1883–1886.

Crane, F.L., Morré, D.J., and Löw, H. (eds) (1988). Plasma Membrane Oxidoreductases in Control of Animal and Plant Growth. (New York: Plenum Press).

Cross, A.R., and Jones, O.T.G. (1986). The effect of the inhibitor diphenylene iodonium on the superoxide-generating system of neutrophils. Specific labeling of a component polypeptide of the oxidase. Biochem. J. **237,** 111–116.

Davis, D., Merida, J., Legendre, L., Low, P.S., and Heinstein, P. (1993). Independent elicitation of the oxidative burst and phytoalexin formation in cultured plant cells. Phytochemistry **32,** 607–611.

Devlin, W.S., and Gustine, D.L. (1992). Involvement of the oxidative burst in phytoalexin accumulation and the hypersensitive reaction. Plant Physiol. **100,** 1189–1195.

Doke, N. (1983). Involvement of superoxide anion generation in the hypersensitive response of potato tuber tissues to infection with an incompatible race of *Phytophthora infestans* and to the hyphal wall components. Physiol. Plant Pathol. **23,** 345–357.

Doke, N. (1985). NADPH-dependent $O_2^{\cdot-}$ generation in membrane fractions isolated from wounded potato tubers inoculated with *Phytophthora infestans.* Physiol. Plant Pathol. **27,** 311–322.

Dwyer, S.C., Legendre, L., Low, P.S., and Leto, T.L. (1996). Plant and human neutrophil oxidative burst complexes contain immunologically related proteins. Biochim. Biophys. Acta **1289,** 231–237.

Fahrendorf, T., Ni, W., Shorrosh, B.S., and Dixon, R.A. (1995). Stress responses in alfalfa (*Medicago sativa* L.). XIX. Transcriptional activation of oxidative pentose phosphate pathway genes at the onset of the isoflavonoid phytoalexin response. Plant Mol. Biol. **28,** 885–900.

Gelli, A., Higgins, V.J., and Blumwald, E. (1997). Activation of plasma membrane Ca^{2+}-permeable channels by race-specific fungal elicitors. Plant Physiol. **113,** 269–279.

Gilroy, S., Read, N.D., and Trewavas, A.J. (1990). Elevation of cytoplasmic calcium by caged calcium or caged inositol triphosphate initiates stomatal closure. Nature **346,** 769–771.

Glaser, B.L., and Brown, D.H. (1955). Purification and properties of D-glucose 6-phosphate dehydrogenase. J. Biol. Chem. **216,** 67–79.

Gout, E., Bligny, R., and Douce, R. (1992). Regulation of intracellular pH values in higher plant cells. J. Biol. Chem. **267,** 13903–13909.

Grabov, A., and Böttger, M. (1994). Are redox reactions involved in regulation of K^+ channels in the plasma membrane of *Limnobium stoloniferum* root hairs? Plant Physiol. **105,** 927–935.

Greenberg, J.T., Guo, A.L., Klessig, D.F., and Ausubel, F.M. (1994). Programmed cell death in plants: A pathogen-triggered response activated coordinately with multiple defense functions. Cell **77,** 551–563.

Greenspan, H.C., and Aruoma, O.I. (1994). Oxidative stress and apoptosis in HIV infection: A role for plant derived metabolites with synergistic antioxidant activity. Immunol. Today **15,** 209–213.

Guern, J., Mathieu, G., Ephritikhine, C.I., Lüttge, U., Marré, M.T., and Marré, E. (1988). Intracellular pH modifications linked to the activity of the ferricyanide driven activity of the plasmalemma redox system in *Elodea densa* leaves, *Acer pseudoplatanus* and *Catharanthus roseus* cells. In Plasma Membrane Oxidoreductase in Control of Animal and Plant Growth, Life Sciences, Vol. 157, F.L. Crane, D.J. Morré, and H. Löw, eds (New York: Plenum Publishing), p. 412.

Guern, J., Mathieu, Y., Kurkdjian, A., Manigault, P., Manigault, J., Gillet, B., Beloeil, J.C., and Lallemand, J.Y. (1989). Regulation of vacuolar pH of plant cells. II. A ^{31}P-NMR study of the modifications of vacuolar pH in isolated vacuoles induced by proton pumping and cation/H^+ exchanges. Plant Physiol. **89,** 27–36.

Guern, J., Felle, H., Mathieu, Y., and Kurkdjian, A. (1991). Regulation of intracellular pH in plant cells. Int. Rev. Cytol. **127,** 111–173.

Hammerschmidt, R., and Kuc, J. (1982). Lignification as a mechanism for induced systemic resistance in cucumber. Physiol. Plant Pathol. **20,** 61–71.

Hatzfeld, W., and Stitt, M. (1990). A study of the rate of recycling of triosephosphates in heterotrophic *Chenopodium rubrum* cells, potato tubers and maize endosperm. Planta **180,** 198–204.

Henderson, L.M., Chappell, J.B., and Jones, O.T.G. (1987). The superoxide-generating NADPH oxidase of human neutrophils is electrogenic and associated with an H^+ channel. Biochem. J. **246,** 325–329.

Isfort, R.J., Cody, D.B., Asquith, T.N., Ridder, G.M., Stuard, S.B., and Leboeuf, R.A. (1993). Induction of protein phosphorylation, protein synthesis, immediate-early-gene expression and cellular proliferation by intracellular pH modulation. Implications for the role of hydrogen ions in signal transduction. Eur. J. Biochem. **213,** 349–357.

Keppler, L.D., and Novacky, A. (1987). The initiation of membrane lipid peroxidation during bacteria-induced hypersensitive reaction. Physiol. Mol. Plant Pathol. **30,** 233–245.

Kieffer, F., Simon-Plas, F., Maume, B.F., and Blein, J.P. (1997). Tobacco cells contain a protein immunologically related to the neutrophil small G protein Rac2 and involved in elicitor-induced oxidative burst. FEBS Lett. **403,** 149–153.

Kohle, H., Young, D.H., and Kauss, H. (1984). Physiological changes in suspension-cultured soybean cells elicited by treatment with chitosan. Plant Sci. **33,** 221–230.

Kuchitsu, K., Kikuyama, M., and Shibuya, N. (1993). *N*-Acetylchitooligosaccharides, biotic elicitors for phytoalexin production, induce transient membrane depolarization in suspension-cultured rice cells. Protoplasma **174,** 79–81.

Levine, A., Tenhaken, R., Dixon, R., and Lamb, C. (1994). H_2O_2 from the oxidative burst orchestrates the plant hypersensitive disease resistance response. Cell **79,** 583–593.

Marré, M.T., Moroni, A., Albergoni, F.G., and Marré, E. (1988). Plasmalemma redox activity and H^+-extrusion. I. Activation of the H^+-pump by ferricyanide-induced potential depolarization and cytoplasm-acidification. Plant Physiol. **87,** 25–29.

Martin, J.B., Bligny, R., Rebeille, F., Douce, R., Leguay, J.J., Mathieu, Y., and Guern, J. (1982). A ^{31}P nuclear magnetic resonance

study of intracellular pH of plant cells cultivated in liquid medium. Plant Physiol. **70,** 1156–1161.

Mathieu, Y., Kurkdjian, A., Xia, H., Guern, J., Koller, A., Spiro, M.D., Oneill, M., Albersheim, P., and Darvill, A. (1991). Membrane responses induced by oligogalacturonides in suspension-cultured tobacco cells. Plant J. **1,** 333–343.

Mathieu, Y., Sanchez, F.J., Droillard, M.J., Lapous, D., Lauriere, C., and Guern, J. (1996a). Involvement of protein phosphorylation in the early steps of transduction of the oligogalacturonide in tobacco cell signal cells. Plant Physiol. Biochem. **34,** 399–408.

Mathieu, Y., Lapous, D., Thomine, S., Lauriere, C., and Guern, J. (1996b). Cytoplasmic acidification as an early phosphorylation-dependent response of tobacco cells to elicitors. Planta **199,** 416–424.

Mehdy, M.C. (1994). Active oxygen species in plant defense against pathogens. Plant Physiol. **105,** 467–472.

Milat, M.L., Ricci, P., Bonnet, P., and Blein, J.P. (1991). Capsidiol and ethylene production by tobacco cells in response to cryptogein, an elicitor from *Phytophthora cryptogea.* Phytochemistry **30,** 2171–2173.

Mittler, R., Shulaev, V., and Lam, E. (1995). Coordinated activation of programmed cell death and defense mechanisms in transgenic tobacco plants expressing a bacterial proton pump. Plant Cell **7,** 29–42.

Nishihara, T., Akifusa, S., Koseki, T., Kato, S., Muro, M., and Hanada, N. (1995). Specific inhibitors of vacuolar type H^+-ATPases induce apoptotic cell death. Biochem. Biophys. Res. Commun. **212,** 255–262.

Nürnberger, T., Nennstiel, D., Jabs, T., Sacks, W.R., Hahlbrock, K., and Scheel, D. (1994). High affinity binding of a fungal oligopeptide elicitor to parsley plasma membranes triggers multiple defense responses. Cell **78,** 449–460.

Ojalvo, I., Rokem, J.S., Navon, G., and Goldberg, I. (1987). ^{31}P NMR study of elicitor-treated *Phaseolus vulgaris* cell suspension cultures. Plant Physiol. **85,** 716–719.

Petitot, A.S., Blein, J.P., Pugin, A., and Suty, L. (1997). Cloning of two plant cDNAs encoding a β-type proteasome subunit and a transformer-2-like SR-related protein: Early induction of the corresponding genes in tobacco cells treated with cryptogein. Plant Mol. Biol. **35,** 261–269.

Ricci, P., Bonnet, P., Huet, J.C., Sallantin, M., Beauvais-Cante, F., Bruneteau, M., Billard, V., Michel, G., and Pernollet, J.C. (1989). Structure and activity of proteins from pathogenic fungi *Phytophthora* eliciting necrosis and acquired resistance in tobacco. Eur. J. Biochem. **183,** 555–563.

Roberts, J.K.M., and Jardetzky, O. (1981). Monitoring of cellular metabolism by NMR. Biochim. Biophys. Acta **639,** 53–76.

Roberts, J.K.M., Aubert, S., Gout, E., Bligny, R., and Douce, R. (1997). Cooperation and competition among adenylate kinase, nucleoside diphosphokinase, electron transport, and ATP synthase in plant mitochondria studied by ^{31}P-nuclear magnetic resonance. Plant Physiol. **113,** 191–199.

Roby, C., Martin, J.B., Bligny, R., and Douce, R. (1987). Biochemical changes during sucrose deprivation in higher plant cells. J. Biol. Chem. **262,** 5000–5007.

Rossi, F. (1986). The $O_2^{\cdot-}$-forming NADPH oxidase of the phagocytes: Nature, mechanisms of activation and function. Biochim. Biophys. Acta **853,** 65–89.

Rubinstein, B., and Stern, A.I. (1986). Relationship of transplasmalemma redox activity to proton and solute transport by roots of *Zea mays.* Plant Physiol. **80,** 805–811.

Satre, M., Martin, J.B., and Klein, G. (1989). Methylphosphonate as a ^{31}P-NMR probe for intracellular pH measurements in *Dictyostelium amoebae.* Biochimie **71,** 941–948.

Schroeder, J.I. (1995). Anion channels as central mechanisms for signal transduction in guard cells and putative functions in roots for plant-soil interactions. Plant Mol. Biol. **28,** 353–361.

Schroeder, J.I., and Hagiwara, S. (1989). Cytosolic calcium regulates ion channels in the plasma membrane of *Vicia faba* guard cells. Nature **338,** 427–430.

Schroeder, J.I., and Hedrich, R. (1989). Involvement of ion channels and active transport in osmoregulation and signaling of higher plant cells. Trends Biochem. Sci. **14,** 187–192.

Schroeder, J.I., Schmidt, C., and Shaeffer, J. (1993). Identification of high-affinity slow anion channel blockers and evidence for stomatal regulation by slow anion channels in guard cells. Plant Cell **5,** 1831–1841.

Segal, A.W., and Abo, A. (1993). The biochemical basis of the NADPH oxidase of phagocytes. Trends Biochem. Sci. **18,** 43–47.

Segal, A.W., Geisow, M., Garcia, R., Harper, A., and Miller, R. (1981). The respiratory burst of phagocytic cells is associated with a rise in vacuolar pH. Nature **290,** 406–409.

Simon-Plas, F., Rusterucci, C., Milat, M.L., Humbert, C., Montillet, J.L., and Blein, J.P. (1997). Active oxygen species production in tobacco cells elicited by cryptogein. Plant Cell Environ., in press.

Slayman, C.L., Long, W.S., and Lu, C.Y.H. (1973). The relationship between ATP and an electrogenic pump in the plasma membrane of *Neurospora crassa.* J. Membr. Biol. **14,** 305–337.

Slonczewski, J.L., Rosen, B.P., Alger, J.R., and Macnab, R.M. (1981). pH homeostasis in *Escherichia coli*: Measurement by ^{31}P nuclear magnetic resonance of methylphosphonate and phosphate. Proc. Natl. Acad. Sci. USA **78,** 6271–6275.

Stallaert, V.M., Ducruet, J.M., Tavernier, E., and Blein, J.P. (1995). Lipid peroxidation in tobacco leaves treated with the elicitor cryptogein: Evaluation by high-temperature thermoluminescence emission and chlorophyll fluorescence. Biochim. Biophys. Acta **1229,** 290–295.

Sussman, M.R. (1994). Molecular analysis of proteins in the plant plasma membrane. Annu. Rev. Plant Physiol. Plant Mol. Biol. **45,** 211–234.

Sutherland, M.W. (1991). The generation of oxygen radicals during host plant responses to infection. Physiol. Mol. Plant Pathol. **39,** 79–93.

Suty, L., Blein, J.P., Ricci, P., and Pugin, A. (1995). Early changes in gene expression in tobacco cells elicited with cryptogein. Mol. Plant-Microbe Interact. **8,** 644–651.

Tavernier, E., Stallaert, V., Blein, J.P., and Pugin, A. (1995a). Changes in lipid composition in tobacco cells treated with cryptogein, an elicitor from *Phytophthora cryptogea.* Plant Sci. **104,** 117–125.

Tavernier, E., Wendehenne, D., Blein, J.P., and Pugin, A. (1995b). Involvement of free calcium in action of cryptogein, a proteinaceous elicitor of hypersensitive reaction in tobacco cells. Plant Physiol. **109,** 1025–1031.

Tenhaken, R., Levine, A., Brisson, L.F., Dixon, R.A., and Lamb, C. (1995). Function of the oxidative burst in hypersensitive disease resistance. Proc. Natl. Acad. Sci. USA **92,** 4158–4163.

Thain, J.F., Gubb, I.R., and Wildon, D.C. (1995). Depolarization of tomato leaf cells by oligogalacturonide elicitors. Plant Cell Environ. **18,** 211–214.

Thuleau, P., Ward, J.M., Ranjeva, R., and Schroeder, J.I. (1994). Voltage-dependent calcium-permeable channels in the plasma membrane of a higher plant cell. EMBO J. **13,** 2970–2975.

Vera-Estrella, R., Blumwald, E., and Higgins, V.J. (1993). Non-specific glycopeptide elicitors of *Cladosporium fulvum*—Evidence for involvement of active oxygen species in elicitor-induced effects on tomato cell suspensions. Physiol. Mol. Plant Pathol. **42,** 9–22.

Viard, M.P., Martin, F., Pugin, A., Ricci, P., and Blein, J.P. (1994). Protein phosphorylation is induced in tobacco cells by the elicitor cryptogein. Plant Physiol. **104,** 1245–1249.

Ward, J.M., Pei, Z.M., and Schroeder, J.I. (1995). Roles of ion channels in initiation of signal transduction in higher plants. Plant Cell **7,** 833–844.

Wendehenne, D., Binet, M.N., Blein, J.P., Ricci, P., and Pugin, A. (1995). Evidence for specific, high-affinity binding sites for a proteinaceous elicitor in tobacco plasma membrane. FEBS Lett. **374,** 203–207.

Xing, T., Higgins, V.J., and Blumwald, E. (1997). Race-specific elicitors of *Cladosporium fulvum* promote translocation of cytosolic components of NADPH oxidase to the plasma membrane of tomato cells. Plant Cell **9,** 249–259.

Zimmermann, S., Thomine, S., Guern, J., and Barbier-Brygoo, H. (1994). An anion current at the plasma membrane of tobacco protoplasts shows ATP-dependent voltage regulation and is modulated by auxin. Plant J. **6,** 707–716.

Zimmermann, S., Nürnberger, T., Frachisse, J.M., Wirtz, W., Guern, J., Hedrich, R., and Scheel, D. (1997). Receptor-mediated activation of a plant Ca^{2+}-permeable ion channel involved in pathogen defense. Proc. Natl. Acad. Sci. USA **94,** 2751–2755.